
OVERCOMING PRACTICAL ISSUES OF DEEP ACTIVE LEARNING AND ITS APPLICATIONS ON NAMED ENTITY RECOGNITION

A PREPRINT

Haw-Shiuan Chang¹ Shankar Vembu² Sunil Mohan³ Rheeya Uppaal¹ Andrew McCallum¹

¹University of Massachusetts Amherst, ²Argmix Consulting, ³Chan Zuckerberg Initiative
hschang@cs.umass.edu, shankar@argmix.com, smohan@chanzuckerberg.com,
ruppaal@cs.umass.edu, mccallum@cs.umass.edu

May 25, 2022

ABSTRACT

Existing deep active learning algorithms achieve impressive sampling efficiency on natural language processing tasks. However, they exhibit several weaknesses in practice, including (a) inability to use uncertainty sampling with black-box models, (b) lack of robustness to noise in labeling, (c) lack of transparency. In response, we propose a transparent batch active sampling framework by estimating the error decay curves of multiple feature-defined subsets of the data.

Experiments on four named entity recognition (NER) tasks demonstrate that the proposed methods significantly outperform diversification-based methods for black-box NER taggers and can make the sampling process more robust to labeling noise when combined with uncertainty-based methods. Furthermore, the analysis of experimental results sheds light on the weaknesses of different active sampling strategies, and when traditional uncertainty-based or diversification-based methods can be expected to work well.

Keywords Active Learning · Transparency · Interpretability · Robustness to Labeling Noise · Black-Box Models · Deep Learning · Clustering · Named Entity Recognition

1 Introduction

Deep neural networks achieve state-of-the-art results on many tasks, especially when a large amount of training data is available. Their success highlights the challenges of reducing the cost of label collection on a large scale.

Active learning can be used to select data samples that will most benefit a predictor’s training, reducing the amount of labeled data needed without hurting the predictor’s accuracy. The effectiveness of uncertainty and disagreement-based¹ active learning methods have been demonstrated on several datasets for simpler predictors [1, 2], and more recently also for deep learning predictors [3, 4, 5].

Nevertheless, random sampling is still the most popular method to build new datasets in many domains, e.g., natural language processing [6]. This is due to many practical issues on the deployment of uncertainty-based active sampling [7, 8], including its limited *applicability*, *robustness*, and *transparency*.

Applicability: Uncertainty sampling selects the samples with the lowest prediction confidence of a predictor and collects their labels. However, the prediction uncertainty might be hard to estimate for some complicated models. For example, a relation extraction system is often a pipeline including named entity extraction, entity linking, and sentence classification. Combining the uncertainty of different components is difficult and usually relies on ad-hoc approaches [9]. Another common case is that state-of-the-art commercial software packages or online services might only provide final predictions (i.e., a black-box predictor) [10]. Our first research question is whether a general active learning method can be based only on the prediction from such black-box predictors.

¹In this work, we view disagreement scores as a kind of uncertainty estimation to simplify our discussion.

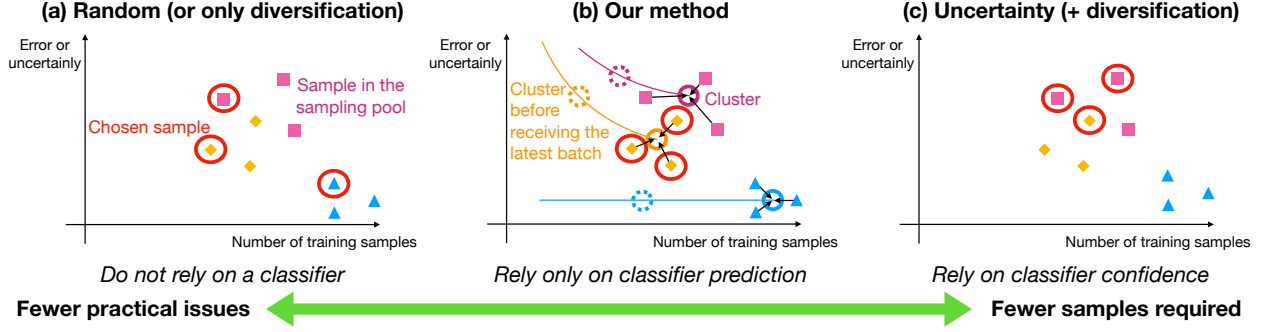


Figure 1: Comparison of sampling strategies. Each node is a word or a sentence in a NER problem and we plot its prediction error/uncertainty versus its count in the current training dataset. Random or diversification-based sampling (a) often selects samples irrelevant to the task, such as a blue triangle node. Uncertainty sampling (c) prefers to select the samples with the highest error/uncertainty (e.g., pink square nodes). However, their error decay could be small because of some inherent label noise. Our method (b) is a novel balance in this spectrum which usually provides better performance than diversification while being more robust, explainable, and applicable than uncertainty sampling (+ diversification).

Robustness: Uncertainty sampling assumes the labels of uncertain examples are the most informative training data. However, the strategy might keep selecting outliers or ambiguous examples for annotators due to their low confidence scores. This selection bias often introduces substantial labeling noise into the dataset [11]. In fact, outlier detection methods often improve the prediction performance by adopting the exactly opposite sample selection strategy compared with uncertainty sampling [12]. It is usually hard to distinguish an informative training data from a misleading outlier, and adopting uncertainty sampling blindly might yield much worse performance than random sampling in practice. Our second research question is whether a general active learning method can be robust to labeling noise without relying on prior knowledge.

Transparency: Active sampling introduces a sampling bias, but we often know little about its effects on the performance in different aspects. This lack of transparency causes many practical issues. Not understanding why an active learning method works well in a dataset, we have few insights about whether the sampling method will work for another similar dataset well enough to compensate the effort of trying active learning, whether the deep predictors will perform worse in some crucial aspects/classes, whether the selection will emphasize undesirable biases (e.g., on a person’s race), and whether the sampling efficiency improvement will vanish in a long run or after switching our deep predictor for uncertainty estimation.

Furthermore, practitioners need to choose a sampling method for a new task and a given deep predictor before collecting labels (e.g., use random, uncertainty, diversification sampling, or combination of the above). Existing deep active learning studies usually focus on prediction performance improvement without exploring why and how much the gain depends on the predictor’s specific ways of modeling feature interaction. The lack of such insights makes the choice extremely difficult [8]. Thus, our third research question is whether we can have a general analysis tool to provide insights into when and why each active sampling works and forecast the potential benefits in different aspects based on a small number of existing labels.

To answer the research questions, we first illustrate 3 kinds of samples in Figure 1. The blue triangle nodes are easy samples, which means their prediction errors are low and stay almost identical if we collect more such labels. The pink square nodes represent the samples with noisy labels, which means their prediction errors or uncertainties are high but reduced slowly as more labels are seen. To select the informative samples like orange diamond nodes, we propose a batch active learning framework that maximizes the error reduction of each sample batch.

In this framework, we propose 3 sampling methods. When we cannot access the uncertainty of the deep predictor but labels of a validation dataset are available, we cluster the samples and predict the validation error reduction on each cluster as shown in Figure 2. The first method is called error decay on groups (EDG). Without a validation dataset, the second method approximates the error decay using prediction changes on groups. Finally, if uncertainty is available, we model the uncertainty reduction of each sample. In the method section, we will describe the first method in details and view the second and third methods as its extensions and denote them as EDG_ext1 and EDG_ext2, respectively.

Analyzing error decay on clusters results in many practical benefits. For example, we can model the error decay using only model prediction, the noisy samples will not be selected due to its low error decay, the strategy of our active

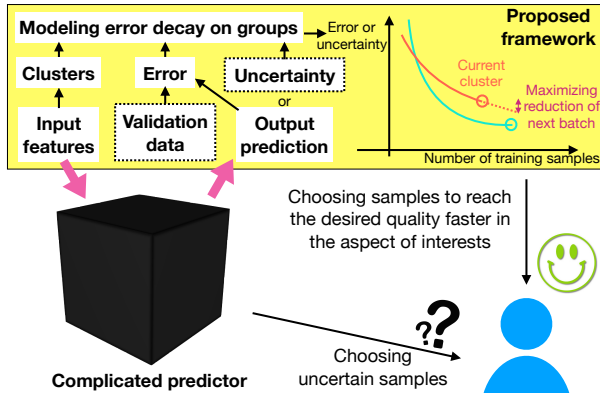


Figure 2: The uncertainty sampling for a black-box predictor is hard to interpret. Our proposed framework predicts the reduction of error/uncertainty on clusters of samples, optionally with the help of validation data. The resulting strategies provide a more direct explanation of the choices made by batch active learning.

	Proposed			Classic	
	EDG	_ext1	_ext2	US (+ Div)	Rnd/Div
Interpretable Strategy	Yes	Yes	No	No	Yes
Robustness to Noise	High	Med	Med	Low	High
Output Required	Pred	Pred	Prob	Prob	None
Validation Required	Yes	No	No	No	No
Label Cost Reduction	Med	Med	High	High	Low

Table 1: Comparison between different sampling approaches. We compare the transparency (i.e., interpretable strategy), robustness to labeling noise, the required output from the predictor, whether the validation data is required, and the cost reduction of collecting clean labels. US means uncertainty sampling (including disagreement-based sampling), Rnd means random sampling, and Div means diversification-based sampling. Med, pred, and prob means medium, predictor prediction, and prediction probability, respectively. In black-box models, only predictions of the predictor are available. The ideal properties are highlighted in the table.

sampling is interpretable (e.g., sampling more uppercase words in a named entity recognition problem due to their larger prediction error decay), and we can predict the performance gain from active learning in different clusters/aspects.

Nevertheless, having only a few labels, we found that achieving the practical advantages sacrifices some sampling efficiency. To feasibly approximate the error reduction, we assume the independence between samples in different clusters. For instance, if a sample is a word in a sentence, our selection method assumes its neighboring words do not affect the error decay of the word. In practice, violation of the assumption causes sub-optimal sampling efficiency compared with uncertainty-based active learning.

The proposed framework is generally applicable to any classification and sequential tagging problems. In the experiments, we focus on named entity recognition (NER) problems where our independence assumption is famously violated to comprehensively evaluate the pros and cons of the proposed methods. We summarize our results in Table 1, which indicate that our framework provides novel ways to trading partial sampling efficiency gain for better *applicability*, *robustness*, and *transparency*.

1.1 Summary of Main Contributions

1. We propose a novel active learning method, EDG, which models validation error decay curves on clusters of samples. We extend the method by replacing validation error decay with prediction difference decay or uncertainty decay to avoid the reliance of validation data. This demonstrates the flexibility of EDG framework.
2. In one synthetic and three real-world NER datasets, we show that EDG significantly outperforms the diversification baseline for the black-box model with or without the help of validation data. This demonstrates the effectiveness and applicability of EDG framework.
3. Modeling the error decay on clusters can be used as an analysis tool for arbitrary active learning methods. The experimental results show that no single method always wins and the proposed analysis tool provides intuitions of why and guidelines of when to select which method. This demonstrates the transparency of EDG framework.
4. We propose a new evaluation method based on pseudo labels. The method allows us to test active learning methods on a large sampling pool and test their robustness to systematic labeling noise.
5. In the experiments on pseudo labels and synthetic dataset, we show that combining EDG with state-of-the-art uncertainty sampling methods (i.e., choosing the samples with the highest uncertainty decay rather than uncertainty) improves the sampling efficiency in the appearance of systematic labeling noise, random labeling noise, and model change. This demonstrates the robustness of EDG framework.

2 Related Work

Several studies aim at making active learning more practical [7]. For example, Phillips, Chang, and Friedler [13] extend the techniques of interpreting a classifier’s prediction to explain the active sampling process, but still rely on the uncertainty estimation of classic machine learning models. Bloodgood and Vijay-Shanker [14] survey and propose stopping criteria based on overall error decay. Instead, we propose novel active sampling by modeling error decay on groups of samples.

Recently, active learning on black-box models has attracted research attention due to practical needs. Wang, Chiticariu, and Li [10] focus on improving a black-box semantic role labeling model using another neural network with low transparency. Rubens et al. [15] propose estimating the variance of prediction of a black-box regressor, which is computationally prohibitive unless applied to simple models such as a linear regressor.

Some approaches, such as Dasgupta [16], cluster input features and diversify samples by choosing them from different clusters, without considering information from the predictors being trained, and often showing only limited improvements in sampling efficiency. Recent approaches [1, 17, 18, 19] have combined uncertainty and diversification (e.g., by multiplying the informativeness score and representativeness score together). By directly modeling the error reduction, our proposed approaches naturally balance the two criteria without relying model uncertainty estimation, which makes our methods robust to labeling noise and applicable to black-box models.

Another direction for deep active learning is to learn an error reduction predictor or a sample selector. However, the selection model is either only applicable to a simple model like naïve Bayes [20, 21], or requires a large amount of data to train a complicated predictor or selector. The training data for the non-transparent selection model usually needs to come from a similar task. For instance, they could be images with different labels for image classification, other users for recommendation, or another language for NER [22, 23, 19]. Although transferring the error reduction predictor between different types of datasets is possible [24], it is unclear on which dataset pairs such a transfer could work.

3 Method

The main goal of batch active learning is to reduce the error $E(C, D_U)$ of a classifier or tagger C on an unseen testing dataset D_U after labeling a fixed number of samples. To simplify the explanation, we first assume that testing error could be well-approximated by validation error and the methods without requiring validation data will be described later as its extensions.

Based on external datasets, previous work maximizes the error reduction by modeling interactions between various types of features such as uncertainty estimation, input features, and the state of the sampling process [24, 22, 23, 19]. In order not to rely on a large external dataset, we first cluster samples based on each feature f into multiple groups, and assume that the validation error of the samples in each group only depends on the number of annotated samples in the same group. Then, estimating the error reduction is decomposed into simple one-dimensional regression problems which can be done by observing only a few pairs of validation errors and its corresponding number of samples.

Specifically, the testing error $E(C, D_U)$ could be partitioned using the sample groups as:

$$E(C, D_U) = \sum_{s_i \in D_U} \sum_{j=1}^{J^f} P(g_j^f | s_i) \sum_{l=1}^{|s_i|} \mathbb{1}(y_{il} \neq \hat{y}_{il}^C), \quad (1)$$

where C is the current predictor, s_i is a sample in the testing data D_U , J^f is the number of groups discovered using feature f , $P(g_j^f | s_i)$ is the probability that the sample s_i belongs to the j th group g_j^f , and $P(g_j^f | s_i)$ could be an indicator function $\mathbb{1}(s_i \in g_j^f)$ if a hard clustering method is used. $\sum_{l=1}^{|s_i|} \mathbb{1}(y_{il} \neq \hat{y}_{il}^C)$ is the error of sample s_i using predictor C . If every sample is a sentence, $|s_i|$ is the length of the sentence, y_{il} is the ground-truth tag for the l th token in the sentence s_i , \hat{y}_{il}^C is the tag predicted by the predictor C .

By assuming that the error of sample s_i could be approximated by the estimated average error of its groups $\hat{E}(g_j^f, C)$ (i.e., $\sum_{l=1}^{|s_i|} \mathbb{1}(y_{il} \neq \hat{y}_{il}^C) \approx \hat{E}(g_j^f, C) |s_i|$), we estimate the overall error as:

$$\hat{E}^f(C, D_U) = \sum_{j=1}^{J^f} \hat{E}(g_j^f, C) m(g_j^f, D_U), \quad (2)$$

where $m(g_j^f, D_U) = \sum_{s_i \in D_U} P(g_j^f | s_i) |s_i|$ could be viewed as the number of times group g_j^f appears in D_U .

3.1 Error Decay Modeling

Since it is undesirable to retrain neural networks many times to get the training data for building a complicated and uninterpretable model, we assume that the error of predictor C_{T_t} on j th group $\hat{E}(g_j^f, C_{T_t})$ is a one-dimensional function $e(n)$, where $n = m(g_j^f, T_t)$ is the number of times group g_j^f appears in the training data T_t after t th batch is collected, and further constrain the class of decay functions $e(n)$ using prior knowledge of the tasks.

The error decay rate of many tasks have been shown theoretically and empirically to be $1/n^k$ [25] and k is typically between 0.5 and 2 [26], so we model the error decay $\hat{E}(g_j^f, C_{T_t}) = e(m(g_j^f, T_t))$ for NER by a fractional polynomial (see the discussion in supplementary material D):

$$e(n) = c_j + b_j \left(\frac{a_{0.5}}{(a_0 \cdot n)^{0.5}} + \sum_{k=1}^3 \frac{a_k}{(a_0 \cdot n)^k} \right), \quad (3)$$

where $a_{0.5}$, a_{0-3} , b_j , and c_j are parameters to be optimized and we constrain these parameters to be non-negative.

The parameters $a_{0.5}$, a_{0-3} , b_j , and c_j are estimated by solving

$$\arg \min_{\substack{\{a_{0-3}, a_{0.5}, \\ b_j, c_j\} \in \mathbf{R}_{\geq 0}^M}} \sum_{j=1}^{J^f} w_j \sum_{t=1}^{t_m} v_{tj} \left(\hat{E}(g_j^f, C_{T_t}) - \frac{E_j^f(C_{T_t}, D_V)}{m(g_j^f, D_V)} \right)^2, \quad (4)$$

where t_m is the number of annotated batches, $E_j^f(C_{T_t}, D_V) = \sum_{s_i \in D_V} P(g_j^f | s_i) \sum_l \mathbb{1}(y_{il} \neq \hat{y}_{il}^{C_{T_t}})$ is the average error of j th group in validation dataset D_V , w_j and v_{tj} are constant weights (see supplementary material G for details of setting the weights), and $M = 2J^f + 5$ is the number of parameters.

For all the NER datasets we tested, we found that it is reasonable to assume that the ratios between terms are shared parameters across all the groups. Due to the small number of parameters, error decay curves could be modeled by retraining deep neural networks only a few times ($t_m = 5$ when selecting the first batch in our experiments).

3.2 Query Batch Selection

Modeling the error decay on each cluster based on different features could be used as an analysis tool to increase the transparency of existing active learning methods. Such an analysis reveals the weaknesses (i.e., the groups of samples with high validation error) of the current tagger and allows us to estimate the number of samples that need to be collected to reach a desirable error rate.

We propose a novel active learning method to actively address the fixable weaknesses of the tagger discovered by the analysis tool. When a single feature f is used, we select the next batch B by maximizing

$$H^f(B \cup T) = - \sum_j e \left(m(g_j^f, B \cup T) \right) m(g_j^f, D_A), \quad (5)$$

where T is the collected training data, and D_A is the union of the pool of candidate sample, training data T , and validation data D_V , which are used to approximate group occurrence statistics in the testing data D_U . Notice that we use $e(m(g_j^f, B \cup T))$ to approximate $\hat{E}(g_j^f, C_{B \cup T})$, so we prevent retraining the predictor C within each batch selection.

Proposition 1. *Suppose that $\hat{E}(g_j^f, C_{T_t})$ is a twice differentiable, non-increasing, and convex function with respect to $m(g_j^f, T_t)$ for all j , then $H^f(T)$ is non-decreasing and submodular.*

The convexity of $\hat{E}(g_j^f, C_{T_t})$ is a reasonable assumption because the error usually decays at a slower rate as more samples are collected. Since selecting more samples only decreases the value of adding other samples, $H^f(T)$ is submodular (See supplementary material E for a rigorous proof).

Finding the optimal B in (5) is NP-complete because the set cover problem can be reduced to this optimization problem [27], but the submodularity implies that a greedy algorithm could achieve $1 - 1/e$ approximation, which is the best possible approximation for a polynomial time algorithm (up to a constant factor) [28, 27].

When performing multiple clustering based on different features f , we select the next sample in the batch as:

$$\arg \max_{s_i} \left(\prod_{f=1}^F \left(\frac{H^f(\{s_i\} \cup T) - H^f(T)}{|s_i|} + \epsilon \right) \right)^{\frac{1}{F}}, \quad (6)$$

where ϵ is a small smoothness term. We normalize the error reduction $H^f(\{s_i\} \cup T) - H^f(T)$ by the sentence length to avoid the bias of selecting longer sentences as done in previous work [1, 4]. After annotators label the whole batch, we retrain the tagger model and update the error decay prediction by solving (4) before selecting the next batch.

Notice that (6) naturally balances the informativeness and representativeness. From the informativeness perspective, the sample without error decay won't be selected. From the representativeness and diversification perspective, we will decrease the value of choosing a sample in a batch after the samples in the same clusters are selected.

4 Method Extensions

For some applications, a validation set is not large enough to be used to model the error decay curves, and our independent assumption might be too strong. To address this concern, we also test two extensions of our method.

4.1 Prediction Difference Decay

We replace the ground truth labels in (4) with the prediction $\hat{y}_{il}^{C_{T_{t_m}}}$ based on the current training data. That is, our sampling method computes the difference between the current prediction and the previous predictions $C_{T_1}, \dots, C_{T_{t_m-1}}$ in each group and models the decay of the difference to maximize convergence rate of predictions. We denote the method as EDG_ext1 in our experiment.

4.2 Uncertainty or Disagreement Decay

When the uncertainty or disagreement information is available, we can model their decay and choose the sentences with highest uncertainty decay rather than highest uncertainty. To avoid making the independence assumption, we skip the clustering step and assume that future uncertainty decay is proportional to previous uncertainty decay, and set the score of i th sentence to be

$$\min(\max(u_i^{t_p} - u_i^{t_m}, 0), u_i^{t_m}), \quad (7)$$

where $u_i^{t_m}$ is the current uncertainty of i th sentence, and $u_i^{t_p}$ is its previous uncertainty. Notice that we take the minimum between the difference and $u_i^{t_m}$ to ensure that the predicted future uncertainty is always non-negative. The method is denoted as EDG_ext2 in our experiment.

5 Experimental Setup

Named entity recognition (NER) problems are often used as a benchmark to evaluate (deep) active learning methods [1, 4, 5] because they are the foundation for many information extraction tasks, and acquiring tags for each token requires a large amount of human effort.

Unless otherwise stated, we use a four-layer convolutional neural network (CNN) as our tagger [29]². We use the published hyper-parameters for real-world datasets, and simplify the tagger in the synthetic data to decrease the standard deviation of the micro-F1 scores.

5.1 Sampling Strategies

We compare the following sampling methods:

- **Random (RND)**: We select sentences randomly with uniform probability.
- **Error Decay on Groups (EDG)**: This is our method where we optimize Equation (6) using validation data.
- **EDG_ext1 (w/o Val)**: As described in the previous section, we replace the validation error in EDG with the prediction difference.
- **Maximum Normalized Log-Probability (US)**: We use the least confidence sampling [30]. This variant of uncertainty sampling has been shown to be very effective in NER tasks [4].

²We choose to test the methods on CNN because Strubell et al. [29] showed that CNN can achieve performance which is close to the state of the art while being much more efficient than BiLSTM-CRF.

- **Maximum Normalized Log-Probability with Diversification (US + Div)**: We diversify uncertain samples based on sentence embeddings (i.e., the average embedding of its words) [17, 4].
- **Diversification (Div)**: We use the same algorithm as US + Div, except that all samples are equally uncertain.
- **US + Div + EDG_ext2**: The same algorithm as US + Div except uncertainty scores are replaced with their difference in Equation (7).
- **Bayesian Active Learning by Disagreement (BALD)**: Disagreement between forward passes with different dropout [3].
- **BALD + EDG_ext2**: Disagreement scores are replaced with their difference in Equation (7).

5.2 Simulation on Gold Labels

This is one of the most widely used setups to evaluate active learning methods. We compare the performances of the NER tagger that are trained on different training data subsets chosen by different methods. In the supplementary material C, we also compare the performances of applying different active learning methods to BiLSTM-CRF models.

5.2.1 Synthetic dataset

We synthesize a dataset with 100 words; each word could be tagged as one of four entity types or none (not an entity). There are three categories of words. The first category consists of half of the words which are always tagged as none. This setup reflects the fact that a substantial amount of words such as verbs are almost always tagged as none in NER tasks. One-fourth of the words belong to the second category where every word mention has the equal probability of being tagged as one of the entity types or none. In real-word NER tasks, the noisy label assignment might be caused by inherently ambiguous or difficult words. The remaining 25 words are in the third category where the labels are predictable and depend on the other context words (See supplementary material H.1 for more details). In this dataset, each word is a group in our method.

5.2.2 Real-world datasets

We test the active sampling methods on CoNLL 2003 English NER [31], NCBI disease [32], and MedMentions [33] datasets. For MedMentions, we remove highly generic types and only consider the remaining 19 important types as Greenberg et al. [34] did and call this subset MedMentions ST19.

In all the three datasets, the first 30,000 tokens are from randomly sampled sentences. To model error decay, we start from 10,000 tokens and retrain the tagger whenever 5,000 new tokens are added. When evaluating the sampling methods, we start from 30,000 tokens, using a batch size of 10,000. The details on how to cluster samples are provided in the supplementary material F.

5.3 Simulation on Pseudo Labels

In practice, we often observe systematic noise from annotators. The noise could come from some inherently difficult/ambiguous cases in the task or from incapable workers in the crowdsourcing platforms. Thus, we propose a novel evaluation method to test the robustness of different sampling methods in the presence of such noise.

As shown in Figure 3, we first train a high-quality tagger using all the training data and use it to tag a large sampling pool. Then, different active learning methods are used to optimize the tagger trained on these pseudo labels. The micro-F1 is measured by comparing the tagger’s prediction with pseudo labels or gold labels on unseen sentences. The evaluation method also allows us to perform sampling on a much larger sampling pool³, which is usually used in the actual deployment of active learning methods.

We also evaluate sampling methods on two practical variations of the above setting. When collecting gold labels for biomedical NER, annotators often tag the whole abstract at a time, which can only be tested using a large sampling pool. In addition, we use the data collected for optimizing a CNN to train BiLSTM-CRF models, which can be used to test the robustness of active learning methods after switching tagger models [8].

6 Results and Analysis

In Figure 4, we present the predicted error decay curves, which fit the empirical values well especially considering the randomness in the initialization of CNNs. The results of the simulation on gold labels and pseudo labels are shown in Figure 5 and Table 2, respectively.

³Running sampling methods on a large pool is time-consuming, so we only compare the methods after the first batch is collected, i.e., when the size of the training dataset reaches 40,000.

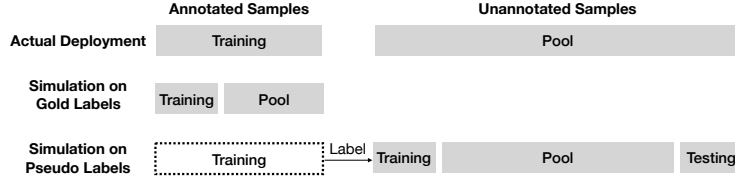


Figure 3: Simulation on pseudo labels compares active learning methods on a large pool with noisy labels. In addition to the original validation and testing set, we also use a testing set with pseudo labels for evaluation.

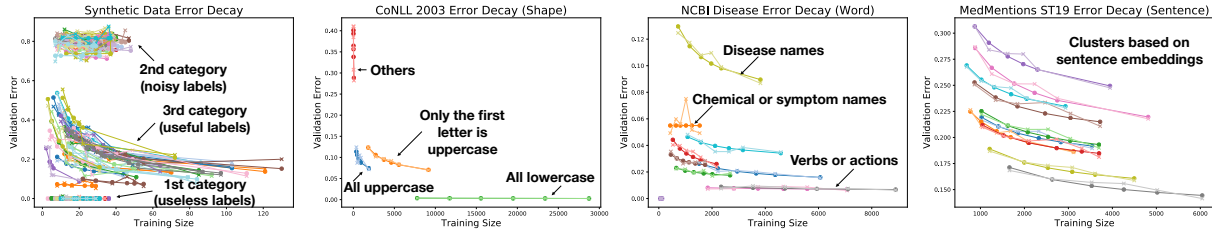


Figure 4: Error decay on groups that are modeled after the first batch is collected by EDG. The points in each curve come from the taggers trained by 10,000, 15,000, 20,000, 25,000, 30,000, and 40,000 words. The x markers on the curves are the real error and ● means prediction from the fitting curve. The groups shown in the figure for NCBI disease and MedMentions ST19 are formed by clustering word and sentence embeddings, respectively.

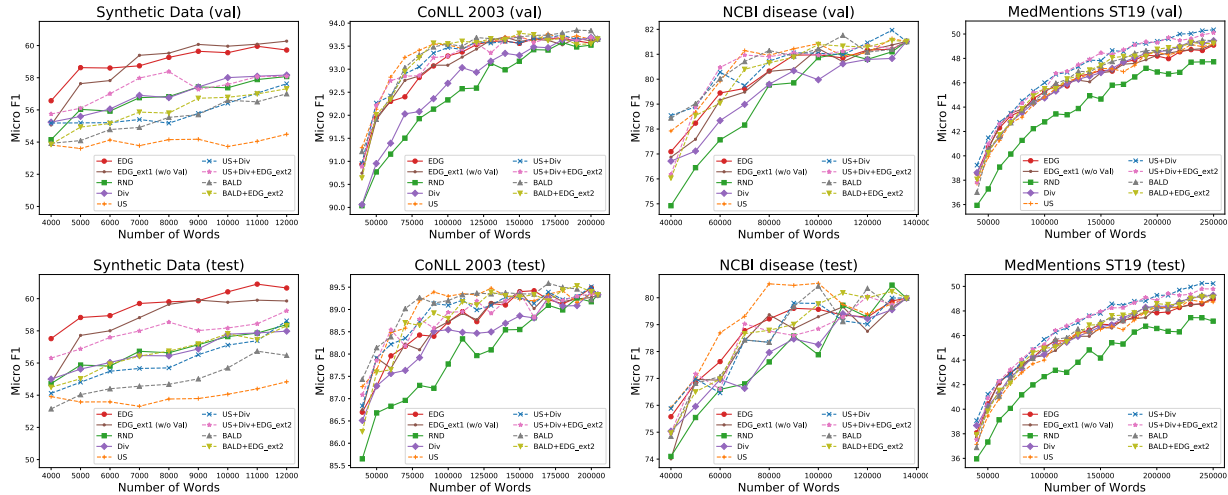


Figure 5: Comparison of different sampling methods on the four NER tasks. The validation (first row) and testing scores (second row) are averaged from the micro-F1 (%) of three CNNs trained with different random initialization. The performance of methods which cannot be applied to black-box taggers is plotted using dotted curves.

6.1 Active Sampling vs Random Sampling

In Figure 4, the error decay curves of both CoNLL 2003 and NCBI disease dataset indicate that there are many uninformative words in these datasets. For example, the lowercase words in CoNLL 2003 are almost never tagged as names of people, organizations, or locations. This explains the findings of Shen et al. [4] that in certain datasets, we can train a neural tagger that reaches a similar performances using only a selected small portion of the training set compared with using all data.

6.2 EDG vs Div and RND

Among the methods we compared against, only random (RND) and diversification (Div) can be applied to black-box taggers. Our method (EDG) significantly outperforms Div and Div outperforms RND in synthetic, CoNLL 2003, and

	Whole abstract						Sentence						Avg
	CNN for CNN			CNN for BiLSTM-CRF			CNN for CNN			CNN for BiLSTM-CRF			
	Val	Test	Pseudo	Val	Test	Pseudo	Val	Test	Pseudo	Val	Test	Pseudo	
EDG [†]	61.0	59.2	54.9	66.5	66.8	58.7	60.1	58.2	54.7	68.2	66.5	59.1	61.2
EDG_ext1 (w/o Val)	59.6	58.5	54.9	65.7	65.5	57.7	60.2	58.4	52.5	67.7	67.8	58.5	60.6
RND	56.0	56.3	50.4	62.6	62.6	55.0	57.7	56.1	52.9	63.9	64.1	56.2	57.8
Div	55.2	55.6	52.8	63.2	63.9	56.1	57.7	56.2	52.5	63.9	64.2	56.6	58.2
US	59.7	59.0	54.1	67.2	67.4	57.8	58.3	57.7	53.1	68.5	68.0	58.1	60.7
US+Div	60.1	59.5	56.0	64.1	65.7	57.9	60.1	56.8	54.5	68.7	67.4	58.5	60.8
US+Div+EDG_ext2	61.2	58.6	56.0	69.5	65.4	58.7	62.2	59.4	55.9	69.8	66.6	58.5	61.8
BALD	59.8	59.4	55.5	67.4	67.7	58.3	59.9	58.8	54.9	69.7	67.3	59.5	61.5
BALD+EDG_ext2	60.7	58.2	56.0	68.4	65.8	58.9	63.7	60.0	54.9	71.7	67.6	59.2	62.1

Table 2: Simulation on pseudo labels for NCBI disease dataset. After selecting the first batch using different sampling methods, the micro-F1 (%) is computed by averaging across five neural networks trained using different random initialization. Whole abstract and sentence mean we sample one abstract and sentence at a time, respectively. CNN for BiLSTM-CRF means that we report the F1 of BiLSTM-CRF that is trained on the data selected for optimizing CNN. The highest score for black-box and uncertainty-based models are highlighted, and the last column shows the unweighted average of all values in each row. The average F1 difference of EDG_ext1 vs Div, US+Div+EDG_ext2 vs US+Div, BALD+EDG_ext2 vs BALD are significant ($p < 0.01$) according to two-sample t-test. [†] indicates the method uses ground truth labels in the validation set to collect samples in the training set.

NCBI disease datasets, which demonstrates the effectiveness of EDG. This also justifies our assumptions and indicates that the error decay curves are modeled well enough for the active sampling purpose.

6.3 US vs US+Div

Shen et al. [4] found that diversification is surprisingly not helpful in batch active learning. However, our results suggest that this finding might be valid only when the sampling pool size is small and/or some groups of frequent words/sentences are clearly not helpful. When the pool is sufficiently large and the task is to jointly extract many different types of entities like MedMentions ST19, sampling almost all kinds of sentences can be helpful to the task as all sentence clusters have the similar decay on the far right of Figure 4. Then, the diversification approach (Div) can be as effective as US and EDG, while US+Div(+EDG_ext2) provides the best result.

6.4 EDG vs Uncertainty-based Methods

As shown in Wang, Chiticariu, and Li [10], it is difficult to perform better in terms of sampling efficiency when comparing a black-box active learning method with uncertainty sampling (US). In real-world datasets, EDG achieves part of the performance gain from US that is easily explainable (e.g., coming from ignoring those easy words), controllable⁴ by humans, and does not involve the specifics of the tagger to model the interaction between each word and its context.

Furthermore, US is not robust to labeling noise or ambiguous samples [11], which have high errors but low error decay. For instance, US almost always selects difficult words with high irreducible errors in the synthetic data. In real-world dataset, we could also observe the ambiguous or difficult words. For example, *insulin* is a chemical, but *insulin resistance* could be a disease or a symptom in NCBI disease dataset. Furthermore, our analysis tool shows that US selects many of such words with incorrect pseudo labels in the supplementary material C.3. The vulnerability makes EDG outperform US in synthetic data and Table 2 on average.

US+Div and BALD are more robust to labeling noise than US, but still suffers from a similar problem. Thus, the sampling strategies that choose more samples with reducible uncertainty (i.e., US+Div+EDG_ext2 and BALD+EDG_ext2) could significantly improve the accuracy of taggers in noisy datasets like our synthetic data and NCBI disease dataset with pseudo labels, while having comparable performance on the other clean datasets with gold labels.

6.5 EDG_ext1 (w/o Val) vs EDG

In all datasets, modeling the error decay using pseudo labels (EDG_ext1) achieves similar performance compared with using gold validation data (EDG) and also outperforms Div.

⁴In the supplementary material C.4, we show that EDG can be easily modified for situations where each label class has a different penalty.

In addition, the micro-F1 scores of EDG on validation and testing data roughly show the similar trend, which suggests that our method does not overfit the validation data even though it has access to its gold labels during sampling.

7 Conclusions

We propose a general active learning framework which is based only on the prediction from black-box predictors, is robust to labeling noise without relying on prior knowledge, and forecasts the potential error reduction in different aspects based on a small number of existing labels.

Our experimental results suggest that no single batch active learning method wins in all the cases which means every method has its own weaknesses. We recommend practitioners to analyze the error decay on groups in order to choose a proper sampling algorithm.

If the sampling pool is small and the above analysis shows that many samples could be easily tagged, then uncertainty sampling methods could be expected to perform well. Otherwise, diversification should be considered or combined with uncertainty sampling. Finally, error decay on groups (EDG) or its extensions should be adopted if we encounter practical deployment challenges such as the issues of *applicability* (e.g., only a black-box predictor is available), *robustness* (e.g., labels are inherently noisy), or *transparency* (e.g., an interpretable sampling process or an error reduction estimation is desired).

8 Acknowledgement

We thank Akshay Krishnamurthy for many helpful discussions. We also thank the anonymous reviewers for their constructive feedback.

This work was supported in part by the Center for Data Science and the Center for Intelligent Information Retrieval, in part by the Chan Zuckerberg Initiative under the project “Scientific Knowledge Base Construction, in part using high performance computing equipment obtained under a grant from the Collaborative R&D Fund managed by the Massachusetts Technology Collaborative, in part by the National Science Foundation (NSF) grant numbers DMR-1534431 and IIS-1514053.

Any opinions, findings and conclusions or recommendations expressed in this material are those of the authors and do not necessarily reflect those of the sponsor.

References

- [1] Burr Settles and Mark Craven. An analysis of active learning strategies for sequence labeling tasks. In *EMNLP*, 2008.
- [2] Burr Settles. Active learning literature survey. *Computer Sciences Technical Report 1648, University of Wisconsin-Madison*, 2009.
- [3] Yarin Gal, Riashat Islam, and Zoubin Ghahramani. Deep bayesian active learning with image data. In *ICML*, 2017.
- [4] Yanyao Shen, Hyokun Yun, Zachary C Lipton, Yakov Kronrod, and Animashree Anandkumar. Deep active learning for named entity recognition. In *ICLR*, 2018.
- [5] Aditya Siddhant and Zachary C Lipton. Deep bayesian active learning for natural language processing: Results of a large-scale empirical study. In *EMNLP*, 2018.
- [6] Katrin Tomanek and Fredrik Olsson. A web survey on the use of active learning to support annotation of text data. In *NAACL HLT 2009 workshop on active learning for natural language processing*, 2009.
- [7] Burr Settles. From theories to queries: Active learning in practice. In *Active Learning and Experimental Design workshop In conjunction with AISTATS 2010*, 2011.
- [8] David Lowell, Zachary C Lipton, and Byron C Wallace. Practical obstacles to deploying active learning. In *EMNLP*, 2019.
- [9] Roi Reichart, Katrin Tomanek, Udo Hahn, and Ari Rappoport. Multi-task active learning for linguistic annotations. In *ACL*, 2008.
- [10] Chenguang Wang, Laura Chiticariu, and Yunyao Li. Active learning for black-box semantic role labeling with neural factors. In *IJCAI*, 2017.

- [11] Stephen Mussmann and Percy Liang. On the relationship between data efficiency and error for uncertainty sampling. In *ICML*, 2018.
- [12] Mohamed-Rafik Bouguelia, Slawomir Nowaczyk, KC Santosh, and Antanas Verikas. Agreeing to disagree: Active learning with noisy labels without crowdsourcing. *International Journal of Machine Learning and Cybernetics*, 9(8):1307–1319, 2018.
- [13] Richard Phillips, Kyu Hyun Chang, and Sorelle A Friedler. Interpretable active learning. In *Conference on Fairness, Accountability and Transparency*, 2018.
- [14] Michael Bloodgood and K Vijay-Shanker. A method for stopping active learning based on stabilizing predictions and the need for user-adjustable stopping. In *CoNLL*, 2009.
- [15] Neil Rubens, Vera Sheinman, Ryota Tomioka, and Masashi Sugiyama. Active learning in black-box settings. *Austrian Journal of Statistics*, 40(1&2):125–135, 2011.
- [16] Sanjoy Dasgupta. Two faces of active learning. *Theoretical computer science*, 412(19):1767–1781, 2011.
- [17] Kai Wei, Rishabh Iyer, and Jeff Bilmes. Submodularity in data subset selection and active learning. In *ICML*, 2015.
- [18] Ozan Sener and Silvio Savarese. Active learning for convolutional neural networks: A core-set approach. In *ICLR*, 2018.
- [19] Sachin Ravi and Hugo Larochelle. Meta-learning for batch mode active learning. In *ICLR workshop*, 2018.
- [20] Nicholas Roy and Andrew McCallum. Toward optimal active learning through Monte Carlo estimation of error reduction. In *ICML*, 2001.
- [21] Weijie Fu, Meng Wang, Shijie Hao, and Xindong Wu. Scalable active learning by approximated error reduction. In *SIGKDD*, 2018.
- [22] Philip Bachman, Alessandro Sordani, and Adam Trischler. Learning algorithms for active learning. In *ICML*, 2017.
- [23] Meng Fang, Yuan Li, and Trevor Cohn. Learning how to active learn: A deep reinforcement learning approach. In *EMNLP*, 2017.
- [24] Ksenia Konyushkova, Raphael Sznitman, and Pascal Fua. Learning active learning from data. In *NIPS*, 2017.
- [25] Joel Hestness, Sharan Narang, Newsha Ardalani, Gregory Diamos, Heewoo Jun, Hassan Kianinejad, Md Patwary, Mostofa Ali, Yang Yang, and Yanqi Zhou. Deep learning scaling is predictable, empirically. *arXiv preprint arXiv:1712.00409*, 2017.
- [26] Shun-ichi Amari, Naotake Fujita, and Shigeru Shinomoto. Four types of learning curves. *Neural Computation*, 4(4):605–618, 1992.
- [27] Andrew Guillory and Jeff Bilmes. Interactive submodular set cover. *arXiv preprint arXiv:1002.3345*, 2010.
- [28] Carsten Lund and Mihalis Yannakakis. On the hardness of approximating minimization problems. *Journal of the ACM (JACM)*, 41(5):960–981, 1994.
- [29] Emma Strubell, Patrick Verga, David Belanger, and Andrew McCallum. Fast and accurate entity recognition with iterated dilated convolutions. In *EMNLP*, 2017.
- [30] Aron Culotta and Andrew McCallum. Reducing labeling effort for structured prediction tasks. In *AAAI*, 2005.
- [31] Erik F Tjong Kim Sang and Fien De Meulder. Introduction to the CoNLL-2003 shared task: Language-independent named entity recognition. In *NAACL*, 2003.
- [32] Rezarta Islamaj Doğan, Robert Leaman, and Zhiyong Lu. NCBI disease corpus: a resource for disease name recognition and concept normalization. *Journal of biomedical informatics*, 47:1–10, 2014.
- [33] Shikhar Murty, Patrick Verga, Luke Vilnis, Irena Radovanovic, and Andrew McCallum. Hierarchical losses and new resources for fine-grained entity typing and linking. In *ACL*, 2018.
- [34] Nathan Greenberg, Trapit Bansal, Patrick Verga, and Andrew McCallum. Marginal likelihood training of bilstm-crf for biomedical named entity recognition from disjoint label sets. In *EMNLP*, 2018.
- [35] Victor S Sheng, Foster Provost, and Panagiotis G Ipeirotis. Get another label? Improving data quality and data mining using multiple, noisy labelers. In *SIGKDD*, 2008.
- [36] Liyue Zhao, Gita Sukthankar, and Rahul Sukthankar. Incremental relabeling for active learning with noisy crowdsourced annotations. In *SocialCom/PASSAT*, 2011.

- [37] Mohamed-Rafik Bouguelia, Yolande Belaïd, and Abdel Belaïd. Stream-based active learning in the presence of label noise. In *4th International Conference on Pattern Recognition Applications and Methods-ICPRAM 2015*, 2015.
- [38] Ashish Khetan, Zachary C Lipton, and Anima Anandkumar. Learning from noisy singly-labeled data. In *ICLR*, 2018.
- [39] Jan Kremer, Fei Sha, and Christian Igel. Robust active label correction. In *International Conference on Artificial Intelligence and Statistics*, 2018.
- [40] Jing Zhang, Xindong Wu, and Victor S Shengs. Active learning with imbalanced multiple noisy labeling. *IEEE transactions on cybernetics*, 45(5):1095–1107, 2015.
- [41] Himabindu Lakkaraju, Ece Kamar, Rich Caruana, and Eric Horvitz. Identifying unknown unknowns in the open world: Representations and policies for guided exploration. In *AAAI*, 2017.
- [42] Irene Chen, Fredrik D Johansson, and David Sontag. Why is my classifier discriminatory? In *Advances in Neural Information Processing Systems*, pages 3543–3554, 2018.
- [43] Burr Settles, Mark Craven, and Soumya Ray. Multiple-instance active learning. In *NIPS*, 2008.
- [44] Jason Baldridge and Miles Osborne. Active learning and the total cost of annotation. In *NIPS*, 2004.
- [45] David Sculley. Web-scale k-means clustering. In *WWW*, 2010.
- [46] Stephen G Nash. Newton-type minimization via the Lanczos method. *SIAM Journal on Numerical Analysis*, 21(4):770–788, 1984.
- [47] Olivier Bodenreider. The unified medical language system (umls): integrating biomedical terminology. *Nucleic acids research*, 32(suppl_1):D267–D270, 2004.
- [48] Ronan Collobert, Jason Weston, Léon Bottou, Michael Karlen, Koray Kavukcuoglu, and Pavel Kuksa. Natural language processing (almost) from scratch. *Journal of Machine Learning Research*, 12(Aug):2493–2537, 2011.
- [49] Tomas Mikolov, Ilya Sutskever, Kai Chen, Greg S Corrado, and Jeff Dean. Distributed representations of words and phrases and their compositionality. In *NIPS*, 2013.
- [50] Wenhui Wang, Nan Yang, Furu Wei, Baobao Chang, and Ming Zhou. Gated self-matching networks for reading comprehension and question answering. In *ACL*, 2017.
- [51] Weiyang Liu, Bo Dai, Xingguo Li, James M Rehg, and Le Song. Towards black-box iterative machine teaching. In *ICML*, 2018.

A Structure of Supplementary Material

We first compare our work with more related work in Section B, and provide more experimental results in Section C.

Then, we describe more technical details of our methods and evaluation, including the discussion of the function choice we used for modeling error decay in Section D, proof of proposition 1 (submodular property) in Section E, the clustering methods used in the experiments in Section F, some other implementation details in Section G, and the details of experiment setups in Section H.

Finally, we discuss some potential future work in Section I.

B Additional Related Work

The proposed framework is flexible and involves various practical issues of active learning, so in our main paper, we cannot cover all the previous studies which address each issue or share methodology similarity in some aspects. To alleviate this concern, we discuss more related work here.

B.1 Robust Active Learning

Popular active learning methods such as uncertainty sampling are not robust to noise [11], so a body of research in active learning is to address this issue. However, the main focus of the previous studies is to identify and post-process the noisy labels given some prior knowledge of the noise-to-signal ratio. Instead, we propose active learning methods which are inherently robust to noise by avoiding the selection of difficult samples for annotators in the first place.

The methods of identify noisy labels are the same or similar to measuring the uncertainty of each samples [35, 12], which could be based on disagreement between workers [35, 36], disagreement between manually created labels and automatically generated predictions [37, 38], model uncertainty [35, 39, 12], or estimation of workers' quality [40, 38].

After the noisy labels are identified, different methods adopt by different strategies such as relabeling [35, 37], excluding/down-weighting the noisy labels [38], or both [36, 40, 12], or acquiring high-quality label using higher costs [39].

B.2 Related Methodology

A challenge related to active learning is to discover blind spots of the predictor (also called unknown unknowns). Lakkaraju et al.[41] view this problem as a multi-armed bandit problem: They first cluster the samples in a pool, and select the samples from a group more often when more unknown unknowns are discovered from the group. However, it is not clear whether the strategy yields better sampling efficiency in terms of the performance of the predictors.

Chen, Johansson, and Sontag[42] define the unfairness as the difference of classification accuracy between two groups and suggest additional data collection as one of the remedies for such unfairness. However, they do not study an active sampling method to efficiently reduce the classification error or the unfairness.

In the extensions we described in the main paper, we maximize the prediction change (i.e., EDG_ext1 in our experiments). The method is related to a type of active learning strategies based on maximizing model change [43, 1, 40]. However, these methods do not address the practical challenges such as transparency, black-box models, and robustness to labeling noise.

C Additional Experimental Results

C.1 CNN for BiLSTM-CRF using Gold Labels

Baldrige and Osborne [44] and Lowell, Lipton, and Wallace [8] demonstrate that the samples collected to optimize one model might not be helpful to another model. To test the robustness of different active learning methods against such model switch, we train BiLSTM-CRF models using the batches collected based on CNN (i.e., CNN for BiLSTM-CRF in Table 2).

The results are presented in Figure 6. Nearly all the observations from Figure 5 also hold in Figure 6. One difference is that EDG and its extensions perform slightly better. For example, in Figure 5 (CNN for CNN setting), BALD+EDG_ext2 sometimes performs slightly worse compared with BALD (e.g., in the testing data of CoNLL 2003 and NCBI disease). However, BALD+EDG_ext2 seems to always perform similar or better (e.g., in MedMentions ST19 and testing data of NCBI disease) than BALD after we switch the tagger model.

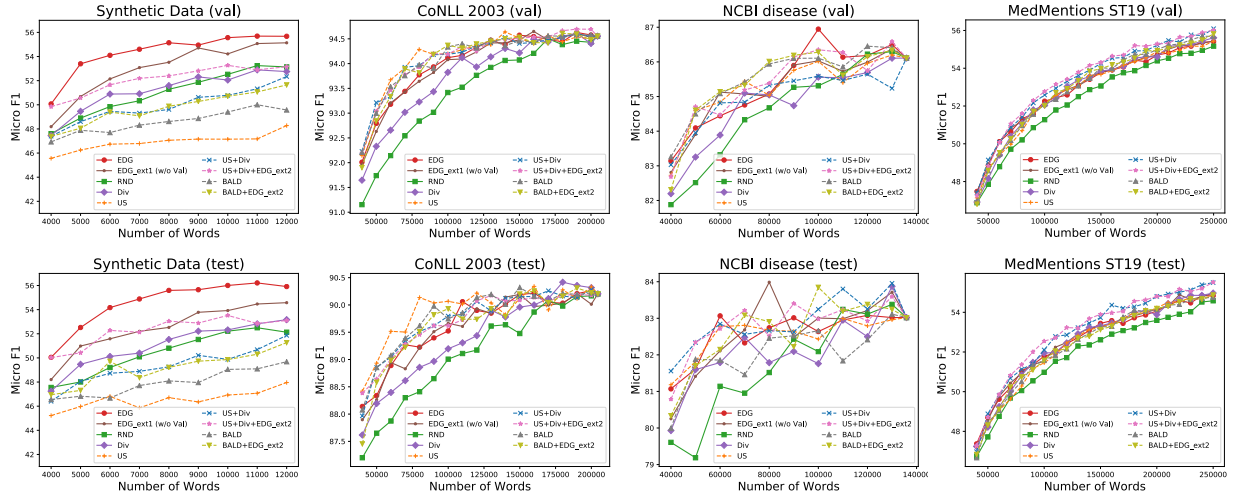


Figure 6: The performance of BiLSTM-CRF models trained on training sets in Figure 5 (i.e., CNN for BiLSTM-CRF setting). The performance metrics are the average micro-F1 (%) of three BiLSTM-CRF trained with different random initialization.

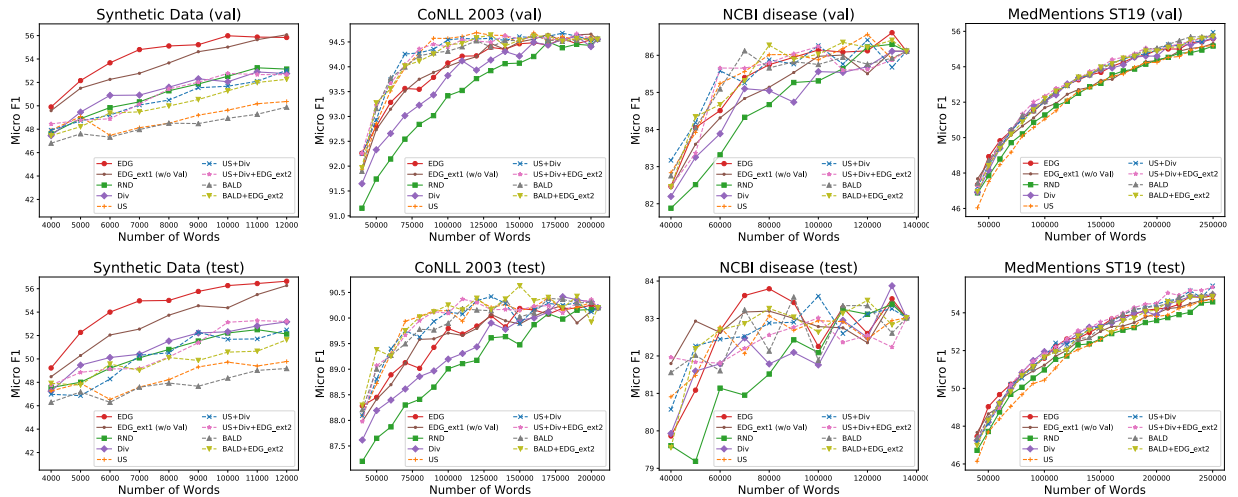


Figure 7: Comparison of applying different sampling methods to BiLSTM-CRF models. The performance metrics are the average micro-F1 (%) of three BiLSTM-CRF trained with different random initialization.

Another difference is that the performance gain between active sampling and random sampling is smaller in MedMentions ST19 than the gap in Figure 5 while we do not observe the similar reduction in CoNLL 2003 and NCBI disease. We hypothesize that active learning methods will skip the groups of unhelpful words in CoNLL 2003 (like lowercase words) and NCBI disease, and those words are usually also unhelpful to other models. Thus, the performance gains in such datasets are more transferable and less depends on the model choice in the first place.

C.2 BiLSTM-CRF for BiLSTM-CRF using Gold Labels

Following Shen et al. [4], we set the uncertainty of each sentence as the negative log likelihood of the predicted label sequence. The results are presented in Figure 7. Most of the observations from Figure 5 also hold in Figure 7. For examples, EDG and its extensions significantly improve the performances in our synthetic dataset, and are significantly better than diversification methods in CoNLL 2003 and NCBI disease datasets. Nevertheless, there are some minor differences. For instances, the performance gap between EDG and uncertainty-based methods is larger in CoNLL 2003, which implies that much sampling efficiency improvement of uncertainty-based methods comes from the specific way

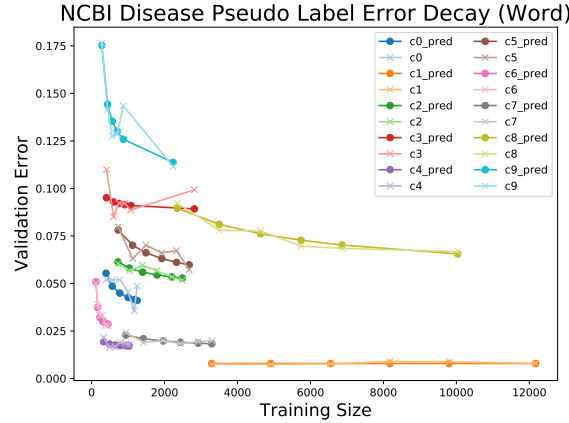


Figure 8: The error decay curves of the taggers trained by pseudo labels in NCBI disease dataset. The six points in each curve come from the taggers trained by 10,000, 15,000, 20,000, 25,000, 30,000, and 40,000 words. The first 30,000 words are selected randomly and uncertainty sampling (US) selects 30,000 – 40,000 words. As in Figure 4, the x markers on the curves are the real error and • means prediction from the fitting curve. The groups are formed by clustering their word embeddings, and the index of each group is presented.

	Whole abstract						Sentence						Avg
	CNN for CNN			CNN for BiLSTM-CRF			CNN for CNN			CNN for BiLSTM-CRF			
	Val	Test	Pseudo	Val	Test	Pseudo	Val	Test	Pseudo	Val	Test	Pseudo	
EDG	61.6	61.9	55.7	68.7	68.2	59.2	62.1	60.2	56.1	70.0	68.2	59.8	62.4
EDG_ext1 (w/o Val)	60.4	61.5	55.4	67.4	67.0	58.6	61.9	60.0	55.2	69.0	69.2	59.1	62.0
RND	56.5	57.9	51.3	64.9	64.1	55.7	58.8	57.2	54.1	65.4	65.2	56.5	59.0
Div	57.9	57.8	54.2	64.4	64.6	57.2	59.3	58.4	53.8	66.2	65.7	57.0	59.7
US	60.9	60.9	54.9	68.1	68.5	58.3	60.0	59.6	54.0	69.7	68.5	59.9	61.9
US+Div	61.1	60.4	56.4	65.4	66.8	58.3	60.5	58.9	55.4	70.1	68.1	59.3	61.7
US+Div+EDG_ext2	61.9	60.1	56.8	71.7	66.1	59.1	63.1	60.8	56.8	70.6	68.6	60.1	63.0
BALD	61.0	61.4	56.4	68.9	69.4	58.8	61.0	59.7	55.1	70.9	67.8	60.1	62.5
BALD+EDG_ext2	61.3	60.0	56.9	69.4	66.5	59.5	65.0	62.2	55.9	72.4	68.7	59.7	63.1

Table 3: The experiment setup is the same as Table 2 except that the performances are the maximal micro-F1 (%) of 5 neural networks rather than their average.

of how the BiLSTM-CRF models dependency between words. In addition, the US and EDG without validation data do not perform well in MedMentions ST19. We hypothesize that this is because the transition probabilities play important roles in this dataset but sampling many uncertain label sequences does not help the BiLSTM model.

C.3 Error Decay of Uncertainty Sampling

The error curve modeling could be used not only to select the next batch but also to analyze the existing sampling strategy. For instance, Figure 8 shows that the last points in the word group 3, 8, and 9 is farther away from the fifth points in x-axis compared with the corresponding distances in other groups. This implies that uncertainty sampling tends to select the samples with the high errors when it chooses the 30,000th to 40,000th tokens as we illustrate in Figure 1. However, the high errors do not necessarily lead to high error reduction in this dataset, which explains that US only achieves 58.3 validation micro-F1 in Table 2, which is significantly worse than other methods like EDG or US+Div.

C.4 Weighted Class Evaluation

To test the controllability of our methods, we set up a variation of MedMentions ST19 where we give different penalties on different classes. Specifically, we focus on 4 related types: *research activity*, *health care activity*, *population group*, and *spatial concept*, and assign 0.9 weights to these classes. Other 15 classes are assigned 0.1 weights. That is, when we compute micro-F1, we weight the total number of correct predictions, the total number of predictions, and the total number of entities according to the importance of classes.

To incorporate the preference into our method, we modify the $E_j^f(C_{T_t}, D_V)$ in Equation (4) as

$$E_j^f(C_{T_t}, D_V) = \sum_{s_i \in D_V} P(g_j^f | s_i) \sum_l \left(\frac{q(y_{il}) + q(\hat{y}_{il}^{C_{T_t}})}{2} \right) \mathbb{1}(y_{il} \neq \hat{y}_{il}^{C_{T_t}}), \quad (8)$$

, where $q(y_{il})$ and $q(\hat{y}_{il}^{C_{T_t}})$ are the weights of the ground truth class and the predicted class.

After this simple modification, our method boosts the weighted micro-F1 in the testing data from 34.3 (using same $q(y)$ for all the classes) to 35.5 (using different $q(y)$ in (4) and (8)) after collecting the first batch in MedMentions ST19 where the score of random sampling is 31.9. The scores come from averaging over the results of 5 random initialization of the CNN.

C.5 Results Statistics

The results do not have high variances in Figure 5. The average standard error in the validation set across all rounds and all the methods are 0.13 for synthetic data, 0.06 for CoNLL 2003, 0.28 for NCBI disease, 0.16 for MedMentions ST19. The average standard error in the testing set are 0.18 for synthetic data, 0.14 for CoNLL 2003, 0.49 for NCBI disease, 0.17 for MedMentions ST19.

In Table 2, we show the average micro-F1 of 5 CNNs with different initialization. Sometimes, we care more about the maximal performance, so we also report the highest F1 score out of 5 runs in Table 3 and the results show a similar trend. When apply two-sample t-test to the comparison of average performance in Table 2, we assume that every micro-F1 score is a true hidden value plus a Gaussian noise, and the variance of the noises are the same given a sampling method. Based on the assumption, the one-tailed two-sample t-test gives us $p < 0.00003$ for the difference between BALD+EDG_ext2 and BALD, between US+Div+EDG_ext2 and US+Div, and between EDG_ext1 and Div.

D Discussion of Functions for Modeling Error Decay Rate

The rate of decay depends on the task [26, 25] and the importance of the context. We discuss the form of error decay functions in one case where context does not affect the label and in the other case where context matters. We hypothesize that the error decay rate of most of the named entity recognition tasks should lie between the decay rate in two cases because the taggers will gradually learn to utilize longer contexts.

Case 1 (Context does not Matter): Assuming we are classifying each token in a sentence into two classes and its label does not depend on context (like predicting a coin toss), we only make reducible errors when we observe the less likely label more times than the other label. Applying Chernoff bound here yields the error decay rate faster than an exponential function.

Without losing the generality, we assume the probability p of observing positive class (i.e., head) in the i th token is smaller than 0.5. Let the number of toss be n and whether the coin is head to be random variable $X_j^i = \mathbb{1}(\text{jth toss on ith coin is head})$. In order to classify the testing tokens optimally (i.e., predict tail whenever seeing the i th token), we would like to observe $X^i = \sum_{j=1}^n X_j^i < \frac{n}{2}$. Therefore, the error rate is $P(X^i \geq \frac{n}{2})(1-p) + p(1 - P(X^i \geq \frac{n}{2})) = P(X^i \geq \frac{n}{2})(1-2p) + p$.

Since all X_j^i are assumed to be independent, we can use Chernoff bounds to model the decay of $P(X^i \geq \frac{n}{2}) = P(X^i \geq (1+\delta)\mu)$ as n increases, where $\mu = p \cdot n$, and $\delta = \frac{0.5-p}{p}$. Chernoff bounds tell us that $P(X^i \geq \frac{n}{2}) \leq \exp(-n \cdot g(p))$, where $g(p)$ is an error decay speed function depend on p . Different versions of Chernoff bounds lead to different $g(\cdot)$, but all $g(\cdot)$ increase as p decreases. That is, when coins are more biased, error rate decay faster.

Case 2 (Context Matters): On the other hand, if we are using naïve Bayes to perform sentiment classification on paragraphs where each word is a group, the error decay function is likely to be as slow as $1/\sqrt{n}$ because determining the label of a paragraph requires the probability of each token indicating the positive class and the error of the probability estimation decay with rate $1/\sqrt{n}$ in the long run according to Chernoff bound or central limit theory.

Recently, Hestness et al. [25] empirically verify that the error decay rate in several important tasks empirically follow $1/n^k$ but k is usually smaller than 0.5. In our experiments on real-world datasets, the error decay rate usually follows the function $1/\sqrt{n}$ when n is large for most of the groups regardless of the feature being used. For example, $a_{0.5}$ in Figure 4 is at least two times larger than the $a_1 + a_2 + a_3$ in CoNLL 2003, NCBI disease, and MedMentions ST19.

E Proof of Proposition 1

We would like to prove $H^f(T) = -\sum_j \hat{E}(g_j^f, C_T)m(g_j^f, D_A)$ is submodular and non-decreasing by assuming $\frac{d\hat{E}(g_j^f, C_T)}{dm(g_j^f, T)} \leq 0$ and $\frac{d^2\hat{E}(g_j^f, C_T)}{d^2m(g_j^f, T)} \geq 0$ for every group g_j^f based on feature f .

First, we prove $-\hat{E}(g_j^f, C_T)$ is submodular and non-decreasing. Assuming we have two subsets X, Z , and one sample s_i such that $X \subseteq Z \subseteq D_A$ and $s_i \in D_A \setminus Z$. Based on the assumption, we can get $m(g_j^f, X) \leq m(g_j^f, Z)$ and $m(g_j^f, X \cup \{s_i\}) \leq m(g_j^f, Z \cup \{s_i\})$ for all g_j^f . Since $\frac{d\hat{E}(g_j^f, C_T)}{dm(g_j^f, T)} \leq 0$, $-\hat{E}(g_j^f, C_T)$ is non-decreasing. In order to consider the case that $m(g_j^f, X \cup \{s_i\}) \geq m(g_j^f, Z)$, we first decompose

$$\begin{aligned} & (-\hat{E}(g_j^f, C_{X \cup \{s_i\}})) - (-\hat{E}(g_j^f, C_X)) \\ &= (-\hat{E}(g_j^f, C_{X \cup \{s_i\}})) - (-\max(\hat{E}(g_j^f, C_{X \cup \{s_i\}}, \hat{E}(g_j^f, C_Z))) \\ & \quad + (-\max(\hat{E}(g_j^f, C_{X \cup \{s_i\}}, \hat{E}(g_j^f, C_Z))) - (-\hat{E}(g_j^f, C_X)), \end{aligned} \quad (9)$$

and

$$\begin{aligned} & (-\hat{E}(g_j^f, C_{Z \cup \{s_i\}})) - (-\hat{E}(g_j^f, C_Z)) \\ &= (-\hat{E}(g_j^f, C_{Z \cup \{s_i\}})) - (-\min(\hat{E}(g_j^f, C_{X \cup \{s_i\}}, \hat{E}(g_j^f, C_Z))) \\ & \quad + (-\min(\hat{E}(g_j^f, C_{X \cup \{s_i\}}, \hat{E}(g_j^f, C_Z))) - (-\hat{E}(g_j^f, C_Z)). \end{aligned} \quad (10)$$

Based on mean value theorem and

$$\begin{aligned} & (-\hat{E}(g_j^f, C_{X \cup \{s_i\}})) - (-\max(\hat{E}(g_j^f, C_{X \cup \{s_i\}}, \hat{E}(g_j^f, C_Z))) \\ &= (-\min(\hat{E}(g_j^f, C_{X \cup \{s_i\}}, \hat{E}(g_j^f, C_Z))) - (-\hat{E}(g_j^f, C_Z)), \end{aligned} \quad (11)$$

we get

$$\begin{aligned} & (-\hat{E}(g_j^f, C_{X \cup \{s_i\}})) - (-\hat{E}(g_j^f, C_X)) - \\ & (-\hat{E}(g_j^f, C_{Z \cup \{s_i\}})) + (-\hat{E}(g_j^f, C_Z)) \\ &= (-\max(\hat{E}(g_j^f, C_{X \cup \{s_i\}}, \hat{E}(g_j^f, C_Z))) \\ & \quad - (-\hat{E}(g_j^f, C_X)) - (-\hat{E}(g_j^f, C_{Z \cup \{s_i\}})) \\ & \quad + (-\min(\hat{E}(g_j^f, C_{X \cup \{s_i\}}, \hat{E}(g_j^f, C_Z))) \\ &= \left(-\frac{d\hat{E}(g_j^f, C_X)}{dm(g_j^f, X)}\Big|_{m(g_j^f, X)=x_1} + \frac{d\hat{E}(g_j^f, C_X)}{dm(g_j^f, X)}\Big|_{m(g_j^f, X)=x_2}\right) \\ & \quad \min(m(g_j^f, Z) - m(g_j^f, X), |s_i|), \end{aligned} \quad (12)$$

where $m(g_j^f, X) < x_1 < \min(m(g_j^f, X \cup \{s_i\}), m(g_j^f, Z))$ and $\max(m(g_j^f, X \cup \{s_i\}), m(g_j^f, Z)) < x_2 < m(g_j^f, Z \cup \{s_i\})$.

Since $x_2 > x_1$ and $\frac{d^2\hat{E}(g_j^f, C_X)}{d^2m(g_j^f, X)} \geq 0$, we know $\frac{d\hat{E}(g_j^f, C_X)}{dm(g_j^f, X)}\Big|_{m(g_j^f, X)=x_1} \leq \frac{d\hat{E}(g_j^f, C_X)}{dm(g_j^f, X)}\Big|_{m(g_j^f, X)=x_2}$, which leads to $(-\hat{E}(g_j^f, C_{X \cup \{s_i\}})) - (-\hat{E}(g_j^f, C_X)) \geq (-\hat{E}(g_j^f, C_{Z \cup \{s_i\}})) - (-\hat{E}(g_j^f, C_Z))$, so $-\hat{E}(g_j^f, C_T)$ is submodular and non-decreasing.

Finally, $H^f(T) = -\sum_j \hat{E}(g_j^f, C_T)m(g_j^f, D_A)$ is submodular and non-decreasing because $m(g_j^f, D_A)$ does not change over X , and the linear combination of submodular and non-decreasing functions with non-negative weights is still submodular and non-decreasing.

F Clustering Features for NER

To simplify the description in Section 3, we assume that the groups are formed by clustering sentences. Nevertheless, the method could also be used to cluster words in sentences. Then, the error in Equation (1) will collapse to $\mathbb{1}(y_i \neq \hat{y}_i^C)$. We need to select a sentence at a time in NER tasks, so in Equation (6), we approximate the error reduction based on the bag of words in each sentence.

	CoNLL 2003		NCBI disease		MedMentions ST19	
	Val	Test	Val	Test	Val	Test
EDG (J=5)	93.0	88.6	79.7	78.5	45.4	44.9
EDG (J=10)	93.1	88.7	80.1	78.4	46.0	45.7
EDG (J=15)	93.1	88.6	79.8	78.3	46.0	45.7
EDG_ext1 (w/o Val) (J=5)	93.0	88.5	79.7	78.5	45.3	44.7
EDG_ext1 (w/o Val) (J=10)	93.1	88.6	80.0	78.1	46.0	45.7
EDG_ext1 (w/o Val) (J=15)	93.0	88.6	79.7	78.7	45.9	45.7

Table 4: Performance sensitivity to the number of clusters (J). Notice that the number of total clusters for the word and word + sentence feature is J^2 (e.g., 225 for $J=15$). The micro-F1 scores (%) are the average over all the training set sizes in Figure 5. The range of training set sizes are 40,000–200,000, 40,000–130,000, 40,000–250,000 for CoNLL 2003, NCBI disease, and MedMentions ST19, respectively. The highest F1 scores using different numbers of clusters for each sampling method are highlighted.

F.1 Clustering Method

For efficiency, all the clustering is done by mini-batch kmeans [45] in D_A , the union of training data, sampling pool, and validation data. We build the 4 sets of groups using different features f .

- Sentence: We compute the sentence embeddings by averaging the word embeddings, and cluster all the sentence embeddings into 10 groups. Next, the cosine similarities between sentence embeddings and the cluster centers are passed through a softmax layer with temperature 0.1 to compute $P(g_j^f | s_i)$.
- Word: We perform a simple top-down hierarchical clustering on word embeddings, which first clusters the word into 10 groups and further partitions each group into 10 clusters. The step results in 100 clusters for words in total.
- Word + Shape: Instead of performing clustering on the lower layer of hierarchical, we partition the words in each group using 4 different word shapes: uppercase letters, lowercase letters, first uppercase letters and rest lowercase letters, other shapes. The same word shape features are also used in our tagger [29].
- Word + Sentence: Similarly, we partition each of the 10 word groups in the lower layer of hierarchy. For each token, we find the sentence s_i the token belongs to, and rely on the sentence group g_j^f with highest $P(g_j^f | s_i)$ to perform partition.

To simplify the method and better control experiment settings, we use the same way to form groups based on the tagger’s input features for all three datasets and use the same groups when selecting all batches in a dataset. Nevertheless, we should note that the framework allows us to model error decay on more fine-grain clusters as more training data are collected, or use other external features (e.g., the journal where the sentence is published) that might not be easily incorporated into the tagger or uncertainty sampling.

F.2 Sensitivity to Number of Clusters

We choose our clustering approach and all other hyper-parameters according to the validation performance after collecting the first batch in CoNLL 2003 and MedMentions ST19, and we find the performance is not sensitive to the choices unless some crucial information is missing (e.g., not considering the word shape in CoNLL 2003). Thus, we fix the number of clusters in each layer to be 10.

In order to verify the claim formally, we report the performances which use different numbers of clusters in each layer in Table 4. We could see that the micro-F1 scores are very close to each other except in the testing set in NCBI disease dataset. We suspect the score variation in NCBI disease mainly comes from the randomness in training process of neural networks because we only conduct one trial of experiments when filling Table 4. The results suggest that cluster number is a trade-off in EDG. Increase the number of clusters decreases the bias but increases the variance in the error decay estimation.

G Implementation Details

In Equation (7), the difference between the current training data size t_m and previous training data size t_p is always 20,000 words for real-world datasets and 2,000 words for the synthetic dataset in our experiments. When choosing samples using Equation (7), we need to be careful about the starvation problem. That is, some types of samples are not selected in the recent history, the samples would have low uncertainty changes which further prevents them from being selected in the future. To mitigate the issue, we alternatively use scores in Equation (7) and the current uncertainty $u_i^{t_m}$

	Synthetic data		CoNLL 2003	
	Token	Sentence	Token	Sentence
Train	99,956	6,726	204,567	14,987
Val	10,045	679	51,578	3,466
Test	10,004	677	46,666	3,684
	NCBI disease		MedMentions ST19	
	Token	Sentence	Token	Sentence
Train	135,900	5,725	758,449	28,227
Val	23,836	941	254,539	9,303
Test	24,255	970	253,737	9,383

Table 5: The size of datasets used in the experiments.

to choose the next batch. For example, when plotting the performance of BALD+EDG_ext2 in Figure 5, we select the first batch using BALD+EDG_ext2 (i.e., Equation (7)) and the second batch using only BALD (i.e., $u_i^{t_m}$), the third batch using BALD+EDG_ext2, and so on. The same strategy is applied to US+Div+EDG_ext2 as well.

In Equation (4), we find that w_j and v_{tj} could be set as 1 in most of the cases. However, we observe some predicted error decay curves collapse into a flat line (i.e., $b_j = 0$ in Equation (3)) due to the unstable performance in validation set. To increase the robustness, we set $w_j = \min(100, m(g_j^f, D_V))$ and $v_{tj} = 3$ if $t = \arg \min_x E_j^f(C_{T_x}, D_V)$ (i.e., lowest error for j th group across t) and $v_{tj} = 1$ otherwise in our experiment, and optimize the Equation (4) using Newton Conjugate-Gradient [46].

In Equation (6), we use geometric mean to combine multiple features because we usually want a sample that has large error reduction on all the groups it belongs to and our preliminary experiments indicate that using geometric mean is better than arithmetic mean. The smoothness constant ϵ in Equation (6) should be proportional to the size of the dataset D_A because larger error reduction could be made in a larger dataset. In the experiment, we set ϵ to be 0.01 for MedMentions ST19 and 0.001 for NCBI disease and CoNLL 2003 dataset.

H Experiment Setting Details

H.1 Synthetic Data

The likelihood of words in the third category being tagged to one of the four entity types is sampled from a Dirichlet distribution with $\alpha_{1-4} = 1$, while the likelihood of being none is zero. Whenever one of these words w appear in the sentence, we check two of its preceding and succeeding words that are also in the third category, average their likelihoods of entity types, and assign the type with the highest likelihood to the word w .

When generating a sentence, the first word is randomly picked. The transition probability within each category is 0.9. Inside the 1st and 2nd categories, the transition probability is uniformly distributed, while the probability of transition to each w inside the 3rd category is proportional to a predetermined random number between $[0.1, 1]$. The sentence length is between $[5, 50]$ and there are 0.1 probability of ending the sentence after generating a word within the range.

The i th word has a word embedding vector $[\mathbb{1}(k = i)]_{k=1}^{100}$. When modeling error decay, we start from 1,000 tokens and use a batch size of 500. When evaluating the sampling methods, we start with 3,000, using a batch size of 1,000. That is, after the first batch is selected, we will update the error decay curves based on the prediction of the taggers trained on 1,000, 1,500, 2,000, 2,500, 3,000 and 4,000 tokens.

H.2 Dataset Preparation and Statistics

CoNLL 2003 datasets have four entity types: people name (PER), organization name (ORG), location name (LOC), and other entities (MISC). In NCBI disease dataset, we only have one type (disease name). The 19 concept types in MedMentions ST19 include *virus*, *bacterium*, *anatomical structure*, *body substance*, *injury or poisoning*, *biologic function*, *health care activity*, *research activity*, *medical device*, *spatial concept*, *biomedical occupation or discipline*, *organization*, *professional or occupational group*, *population group*, *chemical*, *food*, *intellectual product*, *clinical attribute*, and *Eukaryote*. The 19 semantic types are level 3 or 4 (higher means more specific) at UMLS [47]. Any concept mapping to more abstract semantic types is removed as Greenberg et al. [34] did. The size of each dataset is presented in Table 5.

When preparing the simulation experiments on pseudo labels of NCBI disease dataset, we randomly select 100,000 abstracts from PubMed as our new sampling pool, which is around 180 times larger than the pool we used in the simulation on gold labels. Precisely, the sampling pool consists of 24,572,575 words and 921,327 sentences. The testing data with pseudo labels have 2,447,607 tokens and 91,591 sentences.

As shown in Table 2, the scores on the gold validation set, the gold testing set, and the testing set using pseudo labels show a similar trend and most active learning methods do better than random regardless of which test set is used. The observation indicates that the taggers do not overfit the label noise in the training data severely.

H.3 Evaluation Metrics

We follow Strubell et al. [29], who compare all the NER performances using phrase-level micro-F1. Namely, precision and recall are computed by counting the exact boundary and type matching between all predicted phrases and ground truth phrases.

H.4 Tagger Model

The word embeddings for CoNLL 2003 are vectors with 50 dimensions from SENNA [48] and the word embeddings for NCBI disease and MedMentions ST19 are word2vec [49] with 50 dimensions trained on 10% of all PubMed text. Before performing clustering, we normalize all the word embedding vectors such that the L2 distance between two words is equal to 2 times of their cosine distance.

In all the experiments, the number of epochs is chosen using validation data. When training BiLSTM-CRF, we also use the implementation and its default hyper-parameters from Strubell et al. [29] except that we increase the max epochs from 250 to 1000 in the synthetic dataset. In the synthetic dataset, we reduce the number of layers of CNN to 2 because the label only depends on the left 2 words and right 2 words. Furthermore, we change the learning rate from $5 \cdot 10^{-4}$ to 10^{-4} , batch size from 128 to 32, and max epochs from 250 to 1000 to make the performance more stable.

H.5 Batch Selection

Selecting only part of a sentence is not reasonable in NER, so each chosen batch might be slightly larger than the desired batch size. The difference is smaller than the length of the last chosen sentence. Since the desired batch size is set to be large (10,000 words in real-world datasets), the batch size difference between sampling methods is negligible.

In BALD, the sentence disagreement is the average of tokens' disagreement. The prediction disagreement of l th token in i th sentence is computed by $\frac{\sum_{k=1}^K \mathbb{1}(y_{il}^k \neq \text{mode}_k(y_{il}^k))}{K}$. The number of forward passes K is set to 10 in our experiments. We use the default values for the hyperparameters of dropout [29].

When applying maximum normalized log-probability (US) to the CNN model, we select the sentences via $\arg \min_{s_i} \frac{1}{|s_i|} \sum_{l=1}^{|s_i|} \max_{y_{il}} \log P(y_{il})$. We implement the US + Div, also called filtered active submodular selection (FASS), described in Shen et al. [4]. We use cosine similarity to measure the similarity between sentence embeddings. The number of candidate sentences is the batch size times $t = 100$. The ϵ is set to be 0.05.

In the simulation on pseudo labels, we greedily select the abstract with the highest sampling score. For all sampling methods, the sampling score of an abstract is the average of the sampling scores of the sentences in the abstract weighted by the sentence length. That is, the selection criteria view an abstract as a bag of sentences just like that a sentence is considered as a bag of words when clustering is performed on words.

I Future Work

In the experiments, we demonstrate that the proposed methods are more transparent and more robust to labeling noise. Nevertheless, we have not yet applied the method to the tasks other than NER to highlight its wide applicability to arbitrary black-box models. For example, when we annotate a corpus for relation extraction, we usually want to select a document which is informative for the named entity recognizer, entity linker, and sentence classifier. This challenge is also called multi-task active learning [9, 7]. Compared with heuristically combine uncertainty of different models [9], our methods provide more flexibility because it allows us to assign weights on the error reduction of each task and select the next batch by considering all tasks jointly.

In addition to the above pipeline system, question answer (QA) is another example where uncertainty is hard to be estimated. Many reading comprehension models such as pointer networks predict the start position and end position of

the answer in a paragraph [50]. However, higher uncertainty on the position prediction does not necessarily mean the model is uncertain about the answer. It is possible that the correct answer appears in many places in the paragraph and the network points to all the right places with similarly low probability.

We have not compared EDG with the active learning methods that are designed for a specific task to solve a specific practical issue. For example, the active sampling methods proposed in Wang, Chiticariu, and Li [10] are designed for semantic role labeling and focus on the applicability issue (i.e., black-box setting). Due to the difficulty of adapting their methods to NER and making the comparison fair, we leave such comparison as our future work.

Finally, getting the uncertainty from a black-box model is sometimes very expensive. Human students are one of these models [51]. It might not be feasible to ask each student to tell us his/her uncertainty on each exercise before selecting the next exercise for him/her. Our method could potentially be extended to this situation so that we could model the student's improvement speed in each topic only relying on his/her prediction in exams and recommend the exercise in the topics where the student could learn most (i.e., have the largest error decay).